JOURNAL OF CATALYSIS 77, 263–278 (1982)

The Hydrogen–Oxygen Reaction over the Pt(111) Surface: Transient Titration of Adsorbed Oxygen with Hydrogen

JOHN L. GLAND, GALEN B. FISHER, AND EDWARD B. KOLLIN

Physical Chemistry Department, General Motors Research Laboratories, Warren, Michigan 48090

Received October 7, 1981; revised March 25, 1982

The kinetics of the hydrogen–oxygen reaction have been characterized on a Pt(111) surface over the 300–450 K temperature range by titration of adsorbed atomic oxygen with hydrogen in the 1.3×10^{-6} to 1.3×10^{-7} Pa (10^{-8} to 10^{-9} Torr) pressure range. These experiments were performed in an apparatus equipped with Auger electron spectroscopy, low energy electron diffraction, and a multiplexed mass spectrometer used for titration and thermal desorption measurements. The hydrogen–oxygen reaction has been studied by monitoring the water formation rate as a function of time for various temperatures, hydrogen pressures, and initial adsorbed oxygen concentrations. Adsorbed atomic oxygen forms islands of ordered atomic oxygen with a (2×2) structure under the conditions used during these experiments. Hydrogen reacts rapidly with adsorbed atomic oxygen to form water above 300 K. Typically reaction probabilities per incident hydrogen molecule were as high as 0.5 over the temperature range studied. Isotope exchange experiments indicate statistical amounts of HDO are formed during titration of adsorbed oxygen with H_2–D_2 mixtures. This isotope result coupled with low temperature spectroscopic studies (*1*) suggests that water formation proceeds via sequential addition of hydrogen first to adsorbed atomic oxygen, then to adsorbed hydroxyl to form the product water. Neither the concerted atomic hydrogen addition mechanism nor the $H_2(a) + O(a) \rightarrow OH(a) + H(a)$ mechanism can be rigorously excluded, however, several observations suggest they are not major pathways. The titration data indicate that the reaction is basically first order in incident hydrogen over the full range of adsorbed oxygen concentrations. The water formation rate is *not* a unique function of oxygen coverage, but also depends on the initial surface oxygen concentration (the largest oxygen coverage attained before the reaction begins). This result demonstrates that all of the adsorbed atomic oxygen is not available for reaction. A simple reaction model is proposed based on the assumption that the island structure of the adsorbed atomic oxygen limits the availability of oxygen for reaction; this simple model rationalizes the qualitative features of the titration data obtained. The model suggests that the key parameters affecting the behavior of the water formation reaction are the size and shape of the oxygen islands and the availability of adsorbed atomic hydrogen in the reaction zone.

INTRODUCTION

The hydrogen–oxygen reaction is an interesting reaction in terms of developing fundamental understanding of catalytic oxidation reactions. Recently adsorption and desorption of water, oxygen, and hydrogen have been studied on the Pt(111) surface (*2–9*). Molecular water adsorption dominates below the 180 K desorption temperature (*3*). Adsorbed hydroxyl formed by oxidation of adsorbed water with adsorbed atomic oxygen has been characterized on the Pt(111) surface (*3, 4*). Oxygen adsorption on the Pt(111) surface has also been characterized (*5, 6*). The adsorption of hydrogen on the Pt(111) surface has been characterized in detail by several authors (*7–9*). Dissociative hydrogen adsorption occurs even at 90 K on the Pt(111) surface (*9*).

A review of catalytic water formation over the platinum group metals has recently been compiled by Norton (*10*). Several authors have studied the hydrogen–oxygen reaction over platinum foils and single crystals (*11–18*). Many of these authors (*11–15*) suggest that molecular hydrogen reacts with atomic oxygen directly. Low temperature experiments reported in a sep-

0021-9517/82/090263-16$02.00/0

arate paper (*1*) indicate that the water formation can occur on a surface which contains only *atomic* hydrogen and atomic oxygen. This low temperature result unambiguously establishes the existence of a reaction mechanism for water formation from adsorbed *atomic* hydrogen and adsorbed atomic oxygen at low temperature. Several observations made during this work coupled with a number of observations made by other groups strongly suggest that the dominant water formation mechanism even at high temperature is sequential addition of atomic hydrogen first to atomic oxygen then to hydroxyl to form water. Neither the concerted atomic hydrogen addition mechanism nor the $H_2 + O \rightarrow OH + H$ mechanism can be rigorously excluded, however, all the data presently available can be explained by a sequential atomic hydrogen addition mechanism with an intermediate OH species.

Surface hydroxyl has been previously proposed as a stable reaction intermediate during water formation on silica-supported platinum (*20*). The hydroxyl species observed on supported platinum is certainly more stable than the adsorbed hydroxyl we characterized on the Pt(111) surface (*3, 4*) or the hydroxyl intermediate implicated during water formation on noble metals (*1, 3, 19, 21*). Our results suggest the same sort of hydroxyl which has been implicated by molecular beam relaxation studies of the hydrogen–oxygen reaction over the Pd(111) surface (*21*). We postulate (see also Ref. (*1*)) as did Engel and Kuipers (*21*) that the formation of adsorbed hydroxyl is rate limiting. That is, atomic hydrogen addition to adsorbed hydroxyl is more rapid than atomic hydrogen addition to adsorbed atomic oxygen. This reaction sequence causes low surface hydroxyl concentrations under all reaction conditions (*1*).

EXPERIMENTAL

The titration experiments were performed in an ultrahigh vacuum system equipped with several gas inlets, a cylindrical mirror analyzer for Auger electron spectroscopy (AES), a low energy electron diffraction unit (LEED), and a multiplexed mass spectrometer with provisions for digital signal acquisition. The platinum (111) sample was oriented and polished using the usual metallographic techniques. The sample was cleaned by 1400 K oxygen treatments and high temperature annealing. Auger electron spectroscopy was used routinely to verify the cleanliness of the surface. Particular care was taken to ensure the absence of calcium and silicon. No "oxide" could be formed on this surface despite strenuous effort, a further indication that our sample is clean.

A brief description of the primary titration methods used will now be presented. The structure and cleanliness of the Pt(111) surface was first verified by LEED and AES. Various amounts of oxygen were then adsorbed on the Pt(111) surface at 100 K from background. Adsorbed atomic oxygen was formed from this adsorbed molecular oxygen by heating to reaction temperature (300–450 K) at 4.7°/s. After the sample reached reaction temperature, a step change in hydrogen pressure was introduced by rapidly opening a leak valve. The step increase in hydrogen pressure took approximately 0.2 s to complete. Water and hydrogen pressures were monitored with the multiplexed mass spectrometer as a function of time until water formation ceased (50 to 500 s, e.g., Fig. 2). The mass spectrometer data were recorded digitally at a rate of 20 Hz and manipulated digitally to facilitate reduction and graphical presentation of the reduced data. Several complete sets of titration experiments were also obtained using a microchannel plate doser as a collimated hydrogen source. Even though the incident hydrogen fluxes are difficult to estimate and therefore absolute reaction probabilities cannot be estimated reliably, the titration curves obtained confirmed the validity of the background experiments.

RESULTS

A set of thermal desorption spectra for the reactants and products of this reaction system are shown in Fig. 1 to illustrate their thermal stability on the Pt(111) surface. Adsorbed molecular water desorbs in a narrow peak at 180 K as illustrated in Fig. 1, curve a (see also Ref. *2*). Water formed by reaction of adsorbed atomic oxygen and adsorbed atomic hydrogen desorbs as three overlapping peaks at 180, 225, and 275 K as illustrated in Fig. 1, curve b. The residual hydrogen from this water formation experiment desorbs in two overlapping peaks at 220 and 290 K (Fig. 1, curve c), while the residual oxygen begins to desorb above 625 K. The titration experiments shown in Figs. 2–8 were performed over the temperature range 300 to 450 K. In this temperature range the desorption spectra in Fig. 1 indicate that no significant oxygen desorption occurs and little hydrogen accumulation can occur on the surface during the titration

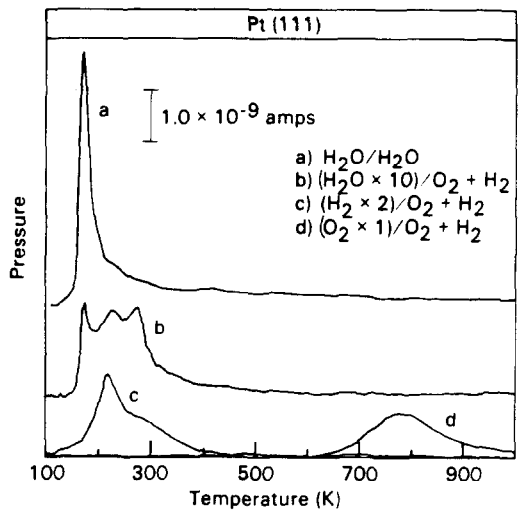

FIG. 1. Two sets of thermal desorption spectra taken after adsorption at 100 K on the Pt(111) surface. (a) Water desorption from a chemisorbed layer of water. (b) Water desorption resulting from reaction between coadsorbed hydrogen and atomic oxygen. (c) Hydrogen desorption from coadsorbed hydrogen and atomic oxygen. (d) Oxygen desorption from coadsorbed hydrogen and atomic oxygen. The heating rate was 4.7°/s.

since hydrogen desorption is rapid. Once molecular water is formed in the 300 to 450 K temperature range it desorbs rapidly from the surface. A complete temperature-programmed reaction study of water formation from adsorbed oxygen and hydrogen on the Pt(111) surface will be reported in a separate paper (*19*).

A series of Auger experiments were performed to verify that all the oxygen-containing species were removed from the surface by titration with hydrogen in the 300 to 450 K temperature range. In all cases no oxygen-containing species remained on the surface after water formation ceased. Therefore, the total amount of water formed during the reaction can be calibrated directly from known initial oxygen concentrations without recourse to estimated vacuum system characteristics (as long as the vacuum system is rapidly pumped). Such a calibration procedure has been used throughout this work. Integrated water rate data from titration of saturated oxygen overlayers [3.8×10^{14} atoms/cm^2 (*5*, *6*)] were checked on a daily basis and the coverage verified with AES [oxygen (510 eV)/Pt(238 eV) = 0.30 ± 0.01 (*5*)]. Reaction probabilities were calculated by dividing the water formation rate by the incident hydrogen flux. As indicated above the water formation rates were obtained by direct calibration of the integrated water formation rate. The hydrogen pressure in the vacuum system was measured using a nude ion gauge and a sensitivity factor of 0.4 relative to N_2.

A series of isotope exchange experiments were performed with a mixture of H_2 and D_2 to ascertain whether hydrogen molecules were reacting directly with the atomic oxygen to form water as has been proposed previously (*11–15*). The results of these experiments are illustrated in Fig. 2. A saturated layer of atomic oxygen was titrated at 400 K with a equimolar mixture of hydrogen and deuterium. Large amounts of the mixed isotope water (HDO) are formed. A substantial kinetic isotope effect is also ob-

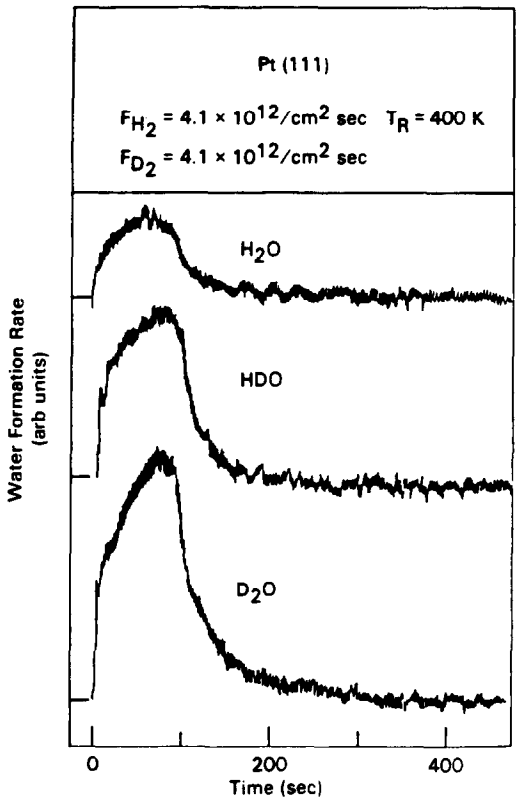

FIG. 2. Titration of an oxygen overlayer with an equimolar mixture of hydrogen molecules and deuterium molecules results in the formation of a large amount of mixed water illustrating that hydrogen dissociation occurs before reaction.

served since D_2 reacts about three times more rapidly than H_2 (Fig. 3). A series of similar experiments were performed for various initial oxygen coverages and hydrogen/deuterium ratios. All the results indicate that a statistical amount of HDO is formed during the titration and a substantial kinetic isotope effect favors reaction of deuterium. In order to verify that the HDO product observed is a direct result of reaction and not a result of the product water exchanging with dissociatively adsorbed hydrogen, several adsorbed layers of atomic oxygen were titrated with H_2 in the presence of a large flux of D_2O at 300 and 400 K. No HDO formation was ever observed indicating that the HDO observed resulted from oxidation of hydrogen.

A set of titration experiments run at 300 K for various initial adsorbed oxygen concentrations are shown in Fig. 3. The left-hand panel of the figure displays the water formation rate as a function of time after baseline subtraction. The right-hand panel of Fig. 3 displays the water formation rate as a function of oxygen surface coverage. Oxygen coverages were determined by integration of the water formation rate as discussed previously. Several sets of titration experiments were run at 300, 400, and 450 K; representative results are shown in Figs. 4, 5, and 6 for 300, 400, and 450 K, respectively. The water formation rate is plotted as a function of oxygen surface concentration for a number of initial adsorbed oxygen concentrations at each temperature. For large initial oxygen concentrations the water formation rate first increases slowly with decreasing oxygen surface concentration then for coverages below about 1.0–1.5

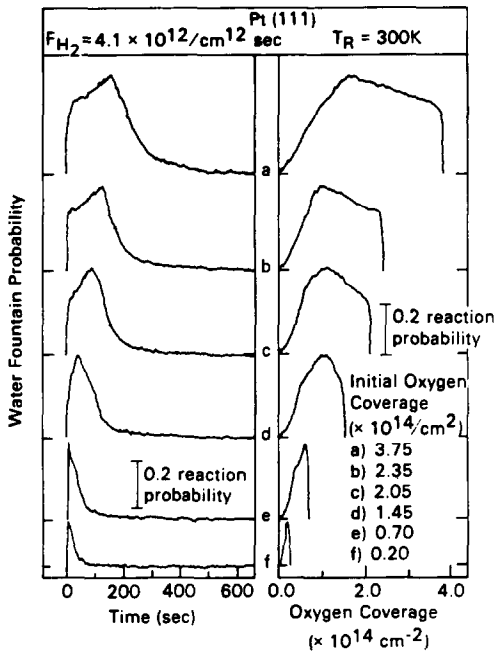

FIG. 3. A set of titration experiments run at 300 K for various initial oxygen concentrations. The data displayed as function of oxygen coverage have been transformed by numerical integration of the rate data as a function of time.

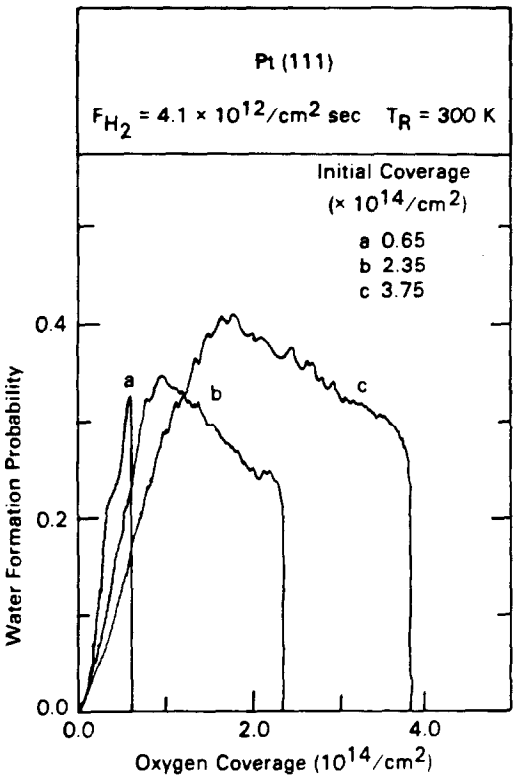

FIG. 4. A set of titration experiments run at 300 K illustrating that the water formation rate is not only a function of oxygen concentration but also depends on the initial oxygen concentration. The incident hydrogen flux is constant through the experiment.

× 10^{14} oxygen atoms/cm^2 the water formation rate decreases rapidly with decreasing oxygen coverage (Figs. 3–6). For small initial oxygen concentrations (below about 1.0 × 10^{14} oxygen atoms/cm^2) the rate decreases rapidly with decreasing oxygen surface concentration (Figs. 3–6). The water formation rate is not a unique function of surface oxygen concentration, but rather depends also on the initial oxygen concentration. For instance, with small oxygen concentrations, the water formation rate is higher for lower initial oxygen concentrations (Figs. 4–6).

In order to characterize the reaction kinetics more completely a series of titration experiments were run for various incident hydrogen fluxes while the initial oxygen coverage and temperature were held constant. The results of these experiments are shown in Figs. 7 and 8 for initial coverages of approximately 3.8 × 10^{14} oxygen atoms/cm^2 and 0.65 × 10^{14} oxygen atoms/cm^2, respectively. Generally the results suggest that the water formation rate is first order with respect to incident hydrogen flux independent of adsorbed oxygen concentration.

A series of LEED observations were made in order to characterize the adsorbed oxygen layer formed on the Pt(111) surface. As indicated in earlier publications (*5, 6*) oxygen islanding is indicated by the appearance of a (2 × 2) overlayer structure far below saturation coverage. Visual observation of a conventional four grid LEED apparatus indicates that the minimum coverage for the appearance of a (2 × 2) overlayer structure during oxygen adsorption at 300 K is approximately 0.6–0.8 × 10^{14} oxygen atoms/cm^2. The (2 × 2) overlayer structure for a saturated oxygen overlayer is quite temperature stable. The (2 × 2) pattern remains quite distinct through

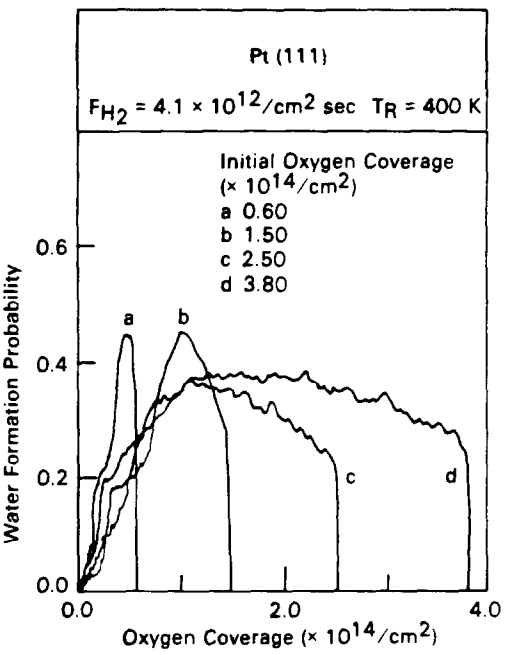

FIG. 5. A set of titration experiments run at 400 K for several initial oxygen coverages with constant incident hydrogen flux.

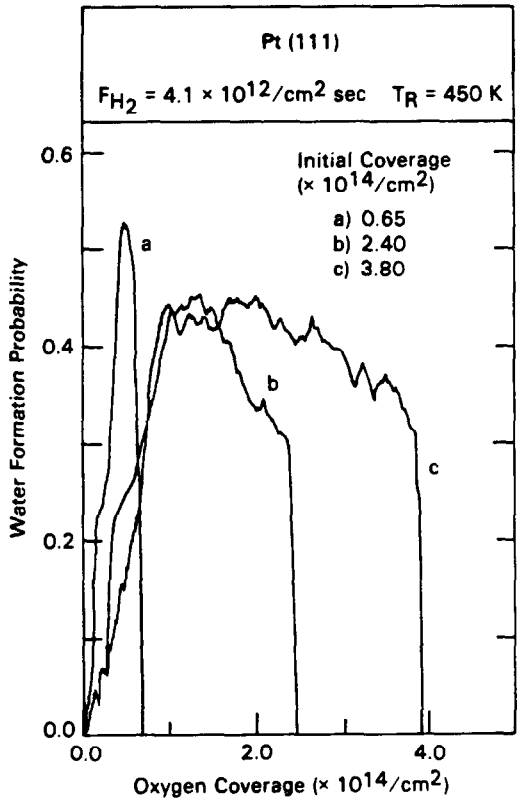

FIG. 6. A set of titration experiments run at 450 K for several initial oxygen coverages with constant incident hydrogen flux.

350–400 K and finally becomes diffuse above 550–600 K. This temperature stability indicates that the oxygen overlayer remains ordered in the temperature range where our titration experiments were run. Direct measurement indicates atomic oxygen surface diffusion begins only above 450 K on the Pt(111) surface (*23*).

DISCUSSION

Reaction Mechanism

Low temperature experiments reported previously indicate that water can be formed by reaction of adsorbed *atomic* hydrogen with atomic oxygen at 120 K (*1*). The isotope reaction results shown in Fig. 2 rule out direct water formation from molecular hydrogen and adsorbed atomic oxygen (an Eley–Rideal mechanism). Several experiments reported in the literature along with kinetic observations made during this work suggest that catalytic water formation on platinum involves a hydroxyl intermediate and sequential addition of adsorbed hydrogen atoms (*3, 4, 17–19, 21*). The evidence which supports this conclusion is reviewed in the next paragraph. However, some of the observations can also be rationalized by postulating the $H_2(a) + O(a) \rightarrow OH(a) + H(a)$ stripping mechanism, by postulating rapid recombination of atomic hydrogen prior to reaction, or by postulating concerted addition of two hydrogen atoms to atomic oxygen. The difficulties encountered in using each of these mechanisms to rationalize the available data are discussed in succeeding paragraphs.

The existence of adsorbed hydroxyl on the Pt(111) surface has recently been demonstrated (*3, 4*). Furthermore, thermal decomposition of a monolayer of adsorbed

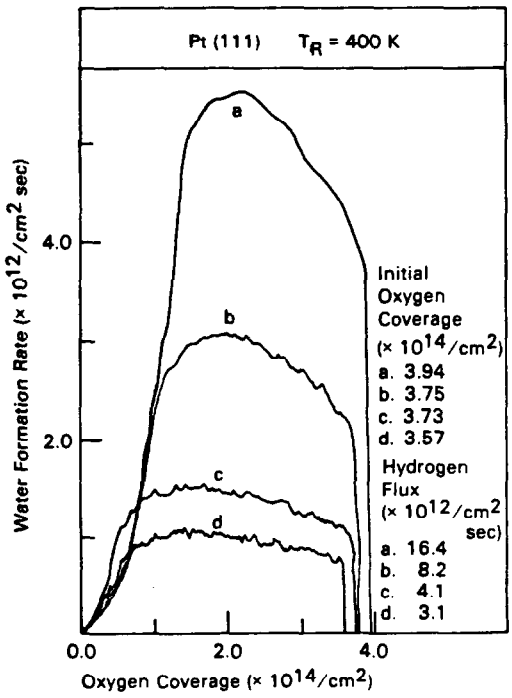

FIG. 7. A set of titration experiments run at 400 K with several incident hydrogen fluxes for a surface saturated with atomic oxygen.

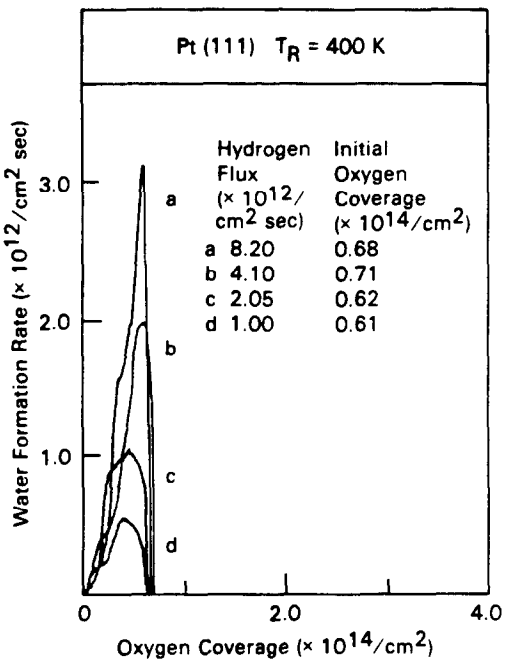

FIG. 8. A set of titration experiments run at 400 K with several incident hydrogen fluxes on a surface with a small initial adsorbed atomic oxygen concentration.

hydroxyl causes a reaction-limited water desorption peak at 200 K indicating water can be formed from adsorbed hydroxyl. During temperature-programmed reaction of coadsorbed atomic hydrogen and atomic oxygen, a reaction-limited water peak is also observed at 200 K (e.g., Fig. 1) suggesting that hydroxyl species may be involved in the reaction. Hydroxyl desorption has also been observed spectroscopically during high temperature water formation from hydrogen and oxygen over platinum gauze (*18*). The translational temperature of water formed by hydrogen–oxygen reaction on a Pt(111) surface is significantly lower than the catalyst surface temperature (*17*). The mechanism which should lead to the smallest exotherm in the final reaction step is clearly addition of adsorbed atomic hydrogen to adsorbed hydroxyl. Finally, a kinetic model which rationalizes *all* the available kinetic data is developed in the next section using a sequential hydrogen atom addition mechanism. The observation that the reaction probabilities observed during titration of adsorbed atomic oxygen with hydrogen (0.5) are substantially higher than the initial sticking coefficient for dissociative hydrogen adsorption on the clean Pt(111) surface (0.1) remains troublesome. In fact, the sticking coefficient for dissociative hydrogen adsorption on an oxygen saturated surface is also 0.1 at 100 K in the absence of chemical reaction (*19*). However, these measured initial adsorption rates for dissociative hydrogen adsorption may be substantially smaller than the actual dissociative adsorption rate because of substantial recombination rates even at low temperature. Substantial recombination rates are reasonable since hydrogen isotope exchange is known to occur even at liquid nitrogen temperature over platinum catalysts.

Two primary difficulties are encountered with the $H_2 + O \rightarrow OH + H$ stripping mechanism. The water formation rate does not decrease with decreasing oxygen coverage over the entire oxygen coverage range as it must if this mechanism is dominant. In this context, the rates for intermediate oxygen coverages are too large. Furthermore, no water formation is observed during hydrogen adsorption on an atomic oxygen covered surface at 100 K. In this situation hydrogen molecules with excess translational energy are certainly incident on adsorbed atomic oxygen, yet no water formation is observed. In contrast, coadsorbed atomic hydrogen and atomic oxygen react readily at 120 K.

A second alternate mechanism involves preliminary dissociative adsorption of hydrogen followed by recombination to form adsorbed molecular hydrogen prior to reaction with adsorbed atomic oxygen. However, the large reaction probabilities observed during water formation strongly suggest that the rate-limiting reaction must be occurring between the two dominant adsorbed species (adsorbed atomic hydrogen and adsorbed atomic oxygen). Two factors

indicate that the concentration of adsorbed molecular hydrogen must be small relative to the concentration of adsorbed atomic hydrogen. The hydrogen recombination rate should be small since the adsorbed atomic hydrogen concentration is small and recombination is a second-order process. The surface lifetime of adsorbed molecular hydrogen must also be very short relative to adsorbed atomic hydrogen because molecular hydrogen is adsorbed very weakly and either desorbs or dissociates rapidly on the surface.

The concerted addition of two adsorbed hydrogen atoms to atomic oxygen is also difficult to accept as a single dominant mechanism. As indicated in our discussion of the sequential mechanism several observations implicate a hydroxyl intermediate which cannot be generated by a concerted mechanism. Furthermore, the large reaction probabilities observed even at low oxygen coverages suggest that two particle collisions should dominate the reaction mechanism since they are much more probable than three particle collisions.

In summary, at the present time we have no data which indicate that more than one mechanism is necessary to rationalize the available data. The most reasonable single mechanism which can be used to rationalize catalytic water formation on platinum is sequential addition of atomic hydrogen first to atomic oxygen then to adsorbed hydroxyl to form water. The other mechanisms discussed cannot be rigorously excluded. The possibility that several reaction mechanisms may be involved in catalytic water formation at various coverages or temperature cannot be disregarded either. However, all the available data can be explained using the simple sequential mechanism indicated below.

$$H_2(\text{gas}) \underset{k_2}{\overset{k_1}{\rightleftarrows}} 2H \qquad (1)$$

$$O + H \xrightarrow{k_3} OH \qquad (2)$$

$$OH + H \xrightarrow{k_4} H_2O(\text{gas}) \qquad (3)$$

These equations are applicable only above the water desorption temperature (180 K). Gas phase species are followed by (gas), all other species are adsorbed on the surface.

Classical Kinetic Model

If we make a series of assumptions these elementary reaction steps can be used to derive reaction rate laws describing the water formation rate in terms of surface concentrations and incident gas flux. If the hydrogen adsorption rate is independent of oxygen coverage and all adsorbed oxygen is reactive, two simple limiting rate laws are obtained depending on the relative rates of hydrogen desorption and reaction. If we apply the steady-state approximation to the adsorbed intermediate species (e.g., OH and H) we obtain:

$$[H] = -\frac{k_3[O]}{2k_2} + \frac{1}{2}\left\{\frac{k_3^2[O]^2}{k_2^2} + \frac{4k_1F_{H_2}}{k_2}\right\}^{1/2}. \qquad (4)$$

The two limiting cases for hydrogen coverage [H] are as follows.

Case I

$$\frac{4k_1F_{H_2}}{k_2} \gg \frac{k_3^2[O]^2}{k_2^2} \qquad (5)$$

Then from (4) we obtain

$$[H] = \left\{\frac{k_1F_{H_2}}{k_2}\right\}^{1/2}. \qquad (6)$$

In this limit the adsorbed hydrogen concentration is determined solely by the hydrogen adsorption and desorption rates since they are larger than the reaction rate. The water formation rate is:

$$\frac{dH_2O}{dt} = k_3[O]\left\{\frac{k_1F_{H_2}}{k_2}\right\}^{1/2}. \qquad (7)$$

Case II

$$\frac{4k_1F_{H_2}}{k_2} \ll \frac{k_3^2[O]^2}{k_2^2}$$

Then from (4) we obtain [H] = O. In this limit the reaction depletes the surface hydrogen concentration since the reaction rate is large. If we examine the behavior of Eq. (4) near [H] = O using a Taylor's expansion we obtain

$$[H] = k_1 F_{H_2}/k_3[O]. \quad (8)$$

The water formation rate is:

$$\frac{d\ H_2O(gas)}{dt} = k_1 F_{H_2}. \quad (9)$$

Thus using the simplest possible rate law which is consistent with our reaction mechanism (*1, 3*) we expect two limiting rate laws depending on the surface oxygen concentration during a titration experiment.

For small oxygen coverages Case I should be appropriate. The rate Eq. (7) indicates first-order dependence on surface oxygen concentration and *half-order* dependence on hydrogen flux. For small oxygen coverages the titration data indicate that the reaction rate is approximately *first order* in surface oxygen coverage (Figs. 3–8). However, the titration data indicate that the reaction is approximately first order in hydrogen flux (Fig. 8) rather than half order as predicted (Eq. (7)).

For large oxygen coverages Case II should be appropriate. The rate Eq. (9) indicates no dependence on surface oxygen concentration and first-order dependence on incident hydrogen flux. For large oxygen coverages the titration data generally agree with these predictions (Figs. 3–8).

Even though the rate laws derived from this simple reaction model can be used to rationalize some of the titration data, there are two major experimental observations which indicate that this model is not realistic. For a given total oxygen surface concentration more than one rate can be observed depending on the initial oxygen concentration (see Figs. 5–7). This observation is rather puzzling since in general kinetic models used to describe surface reactions result in rate expressions which are single valued functions of reactant surface concentrations. Also, for small initial oxygen concentrations the reaction rate observed is approximately first order in incident hydrogen flux (Fig. 8) rather than half order as suggested by Eq. (7). In the following section we will develop a simple reaction model which rationalizes all the available reaction data and is consistent with the experimental data available for oxygen and hydrogen adsorption on the Pt(111) surface.

Hypothesis for Island Reaction Model

The titration data indicate that for a given total oxygen surface concentration several reaction rates can be observed depending on the initial oxygen concentration. One simple way to rationalize this behavior is suggested by the observation that adsorbed atomic oxygen forms ordered islands. Oxygen islands contain two types of adsorbed oxygen atoms, those on the perimeter and those in the interior of the islands. If perimeter oxygen is substantially more reactive than the interior oxygen, the observation that several reaction rates can be observed for a given total surface oxygen concentration can be easily explained. As the oxygen islands grow with increasing oxygen surface coverage the islands touch and some fraction of those which touch merge to form larger islands. Since this coalescence basically changes the fraction of the oxygen which is available for reaction, the reaction rate at a given total oxygen concentration will depend on the initial oxygen coverage.

The experimental data also indicate that the reaction rate is first order in hydrogen flux even in the region where it is also first order in surface oxygen concentration. In the 300 to 450 K temperature region the hydrogen recombination and desorption rate is substantial [Refs. (*7–9*), see also Fig. 1] so that the residence time for hydrogen atoms on the Pt(111) surface must be fairly short. If the reaction between adsorbed oxygen atoms and hydrogen atoms occurs only on the perimeters of oxygen islands, then hydrogen which cannot move to a pe-

rimeter before desorbing cannot react. This hypothesis leads to first-order dependence of the reaction rate on incident hydrogen flux even at low oxygen surface concentrations because the reaction rate is limited by the amount of hydrogen adsorbing near the perimeter oxygen, not by the amount of hydrogen on the entire surface.

In order to illustrate these ideas, a simplified model which takes into account the key factors discussed above is developed in the next section. A series of representative rate expressions are developed to illustrate that the kinetic behavior we observe experimentally can be rationalized using even a simplified reaction model. The primary point we wish to make here is that the data indicate that *not* all of the adsorbed atomic oxygen is available for reaction with adsorbed atomic hydrogen. Consideration of the oxygen island structure can explain these otherwise puzzling data.

Formulation of Island Reaction Model

In order to formulate this reaction model we assume that the adsorption rate of hydrogen near reactive perimeter oxygen limits the reaction rate. Instead of considering the details of surface diffusion driven by concentration gradients on the surface, we assume that all hydrogen which dissociatively adsorbs within a distance "h" of an oxygen perimeter reacts; all other hydrogen desorbs. The "diffusion" length, h, is a model parameter which limits the area for reactive hydrogen adsorption. This parameter may not relate directly to diffusion distances on metal surfaces since modifications of hydrogen mobility or hydrogen recombination rates which may occur in the presence of adsorbed atomic oxygen would affect the reactive adsorption zone area. We further assume that the dissociative hydrogen adsorption rate and the distance "h" are independent of local oxygen concentration.

Oxygen adsorbed in the interior of islands is assumed to be inactive; only oxygen on island perimeters is reactive. All oxygen islands are assumed to have locally saturated oxygen densities and adsorbed oxygen is assumed to be immobile. The idealized oxygen island structure we assume is illustrated in Fig. 9. The reactive hydrogen adsorption zone defined by the length "h" is illustrated by the shaded areas in Fig. 9. Square island symmetry has been used in order to simplify the model since for this case islands formed by coalescence at high coverage do not dramatically change shape as the reaction proceeds (compare Figs. 9e and f). We assume a regular square array of island nucleation centers (Fig. 9a). These nucleation centers are populated by island nuclei with random translational phasing. Four translational domain types can occur for a (2 × 2)O structure on a (111) surface. After population of all the nucleation centers the islands grow uniformly with increasing oxygen surface concentration as indicated in Figs. 9b, c, and d. The four domain types are indicated in Fig. 9 by the four types of cross-hatching. When the islands touch at full coverage, adjacent regions with the same domain type merge, resulting in island growth (Fig. 9e). As the oxygen surface concentration is decreased by reaction at the island perimeters the islands decrease in size as illustrated in Fig. 9f.

Using the assumption outlined in the preceding two paragraphs to describe the situation on the surface a series of expressions describing the reaction rate can be developed. The elementary reaction steps described previously (Eqs. (1)–(3)) are used. However, the reaction rate is limited by the adsorption of hydrogen in the reaction zone. The water formation rate is simply

$$\frac{d\,\mathrm{H_2O(gas)}}{dt} = k_1 F_{\mathrm{H_2}} A \qquad (9)$$

where A is the fraction of the total area which is reactive.

First consider initial oxygen coverages below the density of nucleation centers "j" the reaction zone area is (Fig. 9a).

Case (a). When the nucleation centers

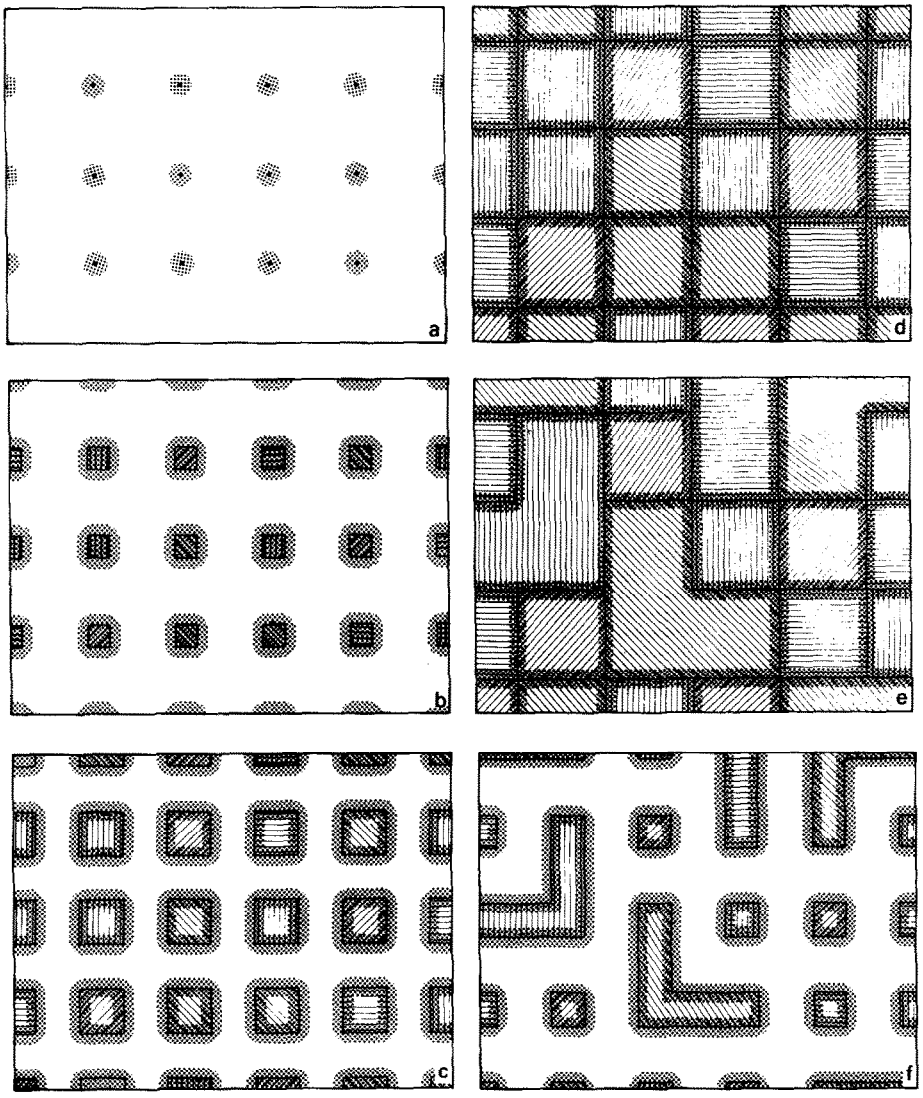

FIG. 9. A set of oxygen island schematics illustrating the simplified island growth and reaction model proposed. The dotted area illustrates an example of the reactive hydrogen adsorption zone. The area occupied by oxygen is cross-hatched with the four directions of cross hatching representing the four translational domains of the (2 × 2)O structure observed on the Pt(111) surface. (a) All oxygen nucleation centers occupied ($[O_T(t)] = [O_s]/64$). (b) Small oxygen islands with interiors included in the reactive adsorption zone ($[(O_T(t)] = [O_s]/16$). (c) Larger oxygen island with part of their interior region not included in the reactive adsorption zone ($[O_T(t)] = [O_s]/4$). (d) A saturated oxygen surface without island coalescence ($[O_T(t)] = [O_s]$). (e) A saturated oxygen island after island coalescence has occurred ($[O_T(t)] = [O_s]$). Note the decrease in reactive adsorption zone area. (f) Oxygen islands formed by removal of oxygen from (e) by reaction ($[O_T(t)] = [O_s]/4$). Note the decrease in reactive zone area compared to (c) which contains the same coverage.

are being populated:

$$\frac{d\,H_2O}{dt} = k_1 F_{H_2} j 4h^2 \frac{O_T(t)}{O_s} \qquad (10)$$

where k_1 is the rate of dissociative hydrogen adsorption, F_{H_2} is the incident flux of hydrogen, h is a "diffusion" distance for atomic hydrogen, j is the density of nuclea-

tion centers or the reciprocal of the maximum island area, O_s is the saturation density of oxygen, and $O_T(t)$ is the total oxygen concentration at time t. The last term in Eq. (10) is simply the fraction of nucleation centers occupied. We have assumed the reaction zone is square (instead of round) so that the form of this equation will match the form of more complex equations derived below.

For larger oxygen coverages we must consider reactive hydrogen adsorption for an oxygen island configuration where the entire oxygen island interior is a reactive hydrogen adsorption zone.

$$A = j\{d(t) + 2h\}^2. \quad (11)$$

The rounded corners of the reactive zone as illustrated in Fig. 9b have been neglected for simplicity. The size of the square oxygen islands, $d(t)$, is directly related to the total oxygen coverage by the equation:

$$jO_s(d(t))^2 = O_T(t). \quad (12)$$

Case (*b*). When the island centers are reactive and the reaction zones do not overlap along their perimeters:

$$\frac{d\,H_2O(gas)}{dt} = k_1 F_{H_2} j \left\{\left(\frac{O_T(t)}{jO_s}\right)^{1/2} + 2h\right\}^2. \quad (13)$$

For larger oxygen coverages the oxygen islands are large enough so that hydrogen adsorbed in the center is inactive, but small enough so the reactive hydrogen adsorption zones are separate. The following fractional reaction zone area is obtained:

$$A = j\{(d(t) + 2h)^2 - (d(t) - 2h)^2\} = j8hd(t). \quad (14)$$

Again we neglect the rounded corners of the reaction zone for simplicity.

Case (*c*). When the island centers are inactive and the reaction zones do not overlap along their perimeters:

$$\frac{d\,H_2O(gas)}{dt} = k_1 F_{H_2} 8jh \left(\frac{O_T(t)}{jO_s}\right)^{1/2}. \quad (15)$$

For oxygen concentrations near saturation we must consider square oxygen islands with overlapping reaction zones.

$$A = j(d(t))^2 - (d(t) - 2h)^2 + ((d_m)^2 - (d(t))^2). \quad (16)$$

Case (*d*). When the island centers are inactive and the reaction zones overlap along their perimeters:

$$\frac{d\,H_2O(gas)}{dt} = k_1 F_{H_2} j \left\{-\frac{O_T(t)}{jO_s} + 4h\left(\frac{O_T(t)}{jO_s}\right)^{1/2} - 4h^2 + d_m{}^2\right\}. \quad (17)$$

Again, we have neglected the rounded corners of the reaction zone for simplicity.

When the oxygen islands reach their maximum size ($d_m = j^{-1/2}$) the islands with similar domain structure will coalesce into larger islands with various configurations. Rate expressions for the major configurations are derived in the appendix. Basically island coalescence reduces the fraction of the oxygen available for reaction if perimeter reaction dominates (compare Figs. 9e and f).

Discussion of Island Reaction Model

The behavior of any one titration experiment as a function of oxygen coverage and hydrogen flux is adequately rationalized by the rate expressions (10), (13), (15), and (17). For instance all these rate expressions indicate first-order dependence of the water formation rate on incident hydrogen flux in agreement with our titration data (Figs. 7 and 8). The negative sign on the highest order oxygen term in Eq. (17) (which describes the reaction rate for large oxygen coverages) indicates that the reaction rate should *increase* with *decreasing* oxygen coverage as was observed at high oxygen coverages (Figs. 3, 4, 5, and 6). Equation (15) indicates that the water formation rate should decrease with a half-order dependence on oxygen coverage and Eqs. (13) and (10) both basically indicate that the water formation rate decreases linearly with

decreasing oxygen coverage. The maximum in the water formation rate observed in Figs. 3–6 for large initial oxygen coverages is suggested by this model as indicated by Eqs. (17) and (15). As the oxygen coverage decreases below the maximum water formation rate the rate first decreases slowly, then decreases linearly with decreasing oxygen coverage as suggested by Eqs. (15), (13), and (10). This comparison indicates that these simple rate expressions can be used to rationalize the functional behavior of any one of these titration experiments. The more complex rate laws derived in the appendix for oxygen overlayers where islands have coalesced display basically the same functional behavior in terms of incident hydrogen flux and also as oxygen coverage decreases during any given titration experiment. The simple coalescence model developed in the appendix suggests that significant decreases in surface reactivity should be expected after the islands coalesce.

The primary point we wish to make here is that the data indicate that not all of the adsorbed atomic oxygen is available for reaction with adsorbed atomic hydrogen. Simple consideration of the oxygen island structure can explain these otherwise puzzling data. We have discussed a simplified reaction model which considers the primary factors which we feel dominate the water formation reaction on the Pt(111) surface. The qualitative agreement between the titration data and this simple reaction model along with known physical characteristics of adsorbed atomic oxygen and adsorbed atomic hydrogen on the Pt(111) surface suggest that the key factors which dominate the hydrogen–oxygen reaction are the structure and size of the oxygen islands and the availability of atomic hydrogen in the reaction zone.

CONCLUSIONS

Hydrogen reacts rapidly with adsorbed oxygen above 300 K to form water. Typical reaction probabilities were as high as 0.3 to 0.5 between 300 and 400 K. Low temperature spectroscopic studies reported separately (*1*) along with isotopic exchange studies reported here suggest that water formation proceeds via sequential addition of adsorbed atomic hydrogen first to adsorbed atomic oxygen then to adsorbed hydroxyl to form the product water. Neither the $H(a) + H(a) + O(a) \rightarrow H_2O(a)$ mechanism nor the $H_2(a) + O(a) \rightarrow OH(a) + H(a)$ mechanism can be rigorously excluded, however, several observations suggest they are not major pathways. The titration data indicate that the reaction is basically first order in incident hydrogen flux. The titration data also indicate that the water formation rate is *not* a unique function of oxygen coverage but also depends on the initial surface oxygen concentration (the largest oxygen coverage attained before reaction begins). This result indicates that all the adsorbed atomic oxygen is not available for reaction. A simple reaction model is proposed based on the assumption that the island structure of the adsorbed atomic oxygen limits the availability of oxygen for reaction; this simple model rationalizes all of the qualitative features of the titration data obtained. The model suggests that the key factors affecting the water formation reaction are the size and shape of oxygen islands and the availability of atomic hydrogen near the reactive oxygen.

APPENDIX

Reaction Model for Coalesced Islands

When the oxygen islands reach maximum size ($d_m = j^{-1/2}$) the islands with similar domain structure will coalesce into larger islands with various configurations. The major configurations are identified in the first column of Table 1. An analytical expression for $d(t)$ in terms of $O_T(t)$ can be obtained by considering simple probability theory. The probability that a given island will have no neighbors of equal domain

TABLE 1

Characteristics of Coalesced Island Configurations

Number of neighboring islands with equivalent domain structure	Configuration probability	Oxygen-covered area as reaction proceeds[a]	Approximate reaction zone area after coalescence[a,b]		
			Island centers reactive, no overlap on perimeters	Island centers inactive, no overlap on perimeters	Island centers inactive, overlapping zones on perimeters
0	0.3164	$d(t)^2$	$d(t)^2 + 4hd(t) + 4h^2$	$8hd(t)$	$-d(t)^2 + 4hd(t) - 4h^2 + d_m^2$
1	0.4219	$\frac{d(t)^2}{2} + \frac{d_m d(t)}{2}$	$\frac{d(t)^2}{2} + 2hd(t) + \frac{d_m d(t)}{2} + hd_m + 2h^2$	$4hd(t) + 2hd_m$	$-\frac{d(t)^2}{2} + 2hd(t) - \frac{d_m d(t)}{2} + hd_m - 2h^2 + d_m^2$
2 (L configuration) included island not the same structure	0.1055	$d_m d(t)$	$d_m d(t) + 2hd_m$	$4hd_m$	$-d_m d(t) + 2hd_m + d_m^2$
2 opposite configuration	0.07031	$d_m d(t)$	$d_m d(t) + 2hd_m$	$4hd_m$	$-2d_m d(t) + 2hd_m + 2d_m^2$
2 (L configuration) included island same structure	0.03516	$\frac{d(t)^2}{4} + \frac{d_m d(t)}{2} + \frac{d_m^2}{4}$	$2hd(t) + 2hd_m$	$2hd(t) + 2hd_m$	$-\frac{d(t)^2}{4} + hd(t) - \frac{d_m d(t)}{2} + hd_m - h^2 + \frac{3d_m^2}{4}$
3 neither included island same structure	0.02637	$\frac{3d_m d(t)}{2} - \frac{d(t)^2}{2}$	$-\frac{d(t)^2}{2} - 2hd(t) + \frac{3d_m d(t)}{2} + 3hd_m - 2h^2$	$-4hd(t) + 6hd_m$	$\frac{d(t)^2}{2} - 2hd(t) - \frac{3}{2}d_m d(t) + 3hd_m + 2h^2 + d_m^2$
3 one included island with same structure	0.01758	$-\frac{d(t)^2}{4} + d(t)d_m + \frac{d_m}{4}$	$-\frac{d(t)^2}{4} - hd(t) + d_m d(t) + 2hd_m - h^2$	$-2hd(t) + 4hd_m$	$\frac{d(t)^2}{4} - hd(t) - d_m d(t) + 2hd_m + h^2 + \frac{3d_m^2}{4}$
3 both included islands with same structure	0.002930	$\frac{d(t)d_m}{2} + \frac{d_m^2}{2}$	$\frac{d_m d(t)}{2} + hd_m$	$2hd_m$	$-\frac{d_m d(t)}{2} + hd_m + \frac{d_m^2}{2}$
4 this low probability configuration is *assumed* to include only dissimilar included island	0.003906	$2d_m d(t) - d(t)^2$	$-d(t)^2 - 4hd(t) + 2d_m d(t) + 4hd_m - 4h^2$	$-8hd(t) + 8hd_m$	$d(t)^2 - 4hd(t) - 2d_m d(t) + 4hd_m + 4h^2 + d_m^2$

[a] Areas have been estimated per nucleation site.

[b] Rounding of the corners of the reaction zone have been neglected.

structure is

$$\frac{(4!)}{(0!)(4!)}(0.25)^0(0.75)^4 = 0.316.$$

In a similar manner the probability that a given island will have a given number of equivalent neighbors in a given configuration can be easily determined and is shown in column 2 of Table 1. The area covered by each type of island configuration and the variation of that area with extent of reaction can also be determined and is shown in column 3 of Table 1 in terms of the maximum island size "d_m" and the current characteristic dimension "$d(t)$". Since we know the probability and the area for each major configuration type, an equation can be developed describing the relationship between total oxygen coverage and the characteristic dimension $d(t)$ of our islands.

$$O_T(t) = jO_s \sum_{\text{configurations}} (\text{configuration probability})(\text{island area}) \quad (18)$$

or

$$d(t) = -0.450\, d_m + 0.955 \left\{0.191\, d_m^2 + 2.094 \left(\frac{O_T(t)}{jO_s}\right)\right\}^{1/2}. \quad (19)$$

In order to estimate the total reactive zone area available for a given total coverage, the reactive zone area available should be estimated for each type of island configuration formed by coalescence. The major types of configurations formed by coalescence are listed in Table 1 along with the reactive areas available for various ranges of the size parameter $d(t)$. As noted in the table, the reactive zone areas have been estimated per nucleation site, and rounding of the corners of the reaction zone has been neglected. For simplicity we have considered only the major configuration for four equivalent neighbors even though there are several different configurations depending on the identity of included corner islands. The population densities of these neglected configurations are less than 0.4% and will have no noticeable effect except for extremely small coverages attained by reacting away the oxygen. The reactive area available for any coverage can now be estimated by determining the characteristic dimension $d(t)$ using Eq. (18) then summing the product of configuration probability and reactive zone area over all the configurations.

$$A = j \sum_{\text{configurations}} (\text{configuration probability})(\text{reaction zone area}). \quad (20)$$

We obtain the following expressions for the fractional reactive areas when the island centers are reactive and the reaction zones do not overlap along their perimeter:

$$A \cong j\{0.5058\, d(t)^2 + 2.094\, hd(t) + 0.4532\, d_m d(t) + 0.9767\, hd_m + 2.023\, h^2\}. \quad (21)$$

When the island center is inactive and the reaction zones do not overlap along their perimeter:

$$A \cong j\{4.117\, hd(t) + 1.883\, hd_m\}. \quad (22)$$

When the island center is inactive and the reaction zones overlap along their perimeter:

$$A \cong j\{-0.5146\, d(t)^2 + 2.059\, hd(t) - 0.5411\, d_m d(t) + 0.9415\, hd_m + 1.056\, d_m^2 - 2.059\, h^2\} \quad (23)$$

where $d(t)$ can be related to oxygen coverage by Eq. (19), h is the "diffusion" length, d_m is the distance between nucleation centers, and j is the nucleation site density.

Complex rate equation describing the reaction rate for coalesced islands can be obtained by first substituting $d(t)$ from Eq. (19) into Eqs. (21), (22), and (23) and then substituting the resulting equations into Eq. (9).

NOMENCLATURE

a Unit cell size for one adsorbed oxygen atom

A The fraction of the total area where reactive hydrogen can adsorb. In our development we calculate the fractional area per island nucleation site

d_m The maximum island size, the distance between nucleation centers (in our model $d_m = j^{-1/2}$)

$d(t)$ Characteristic island size. For independent square islands the overall dimension of the square. For coalesced island configurations the short side dimension which decreases with extent of reaction

F_{H_2} Incident flux of H_2(gas) on the surface

h Adsorbed atomic hydrogen "diffusion" distance, a model parameter which defines the reactive adsorption zone

j Island nucleation site density (in our model $j = 1/d_m^2$)

k_1 Rate constant for hydrogen adsorption

k_2 Rate constant for hydrogen desorption

k_3 Rate constant for reaction of adsorbed atomic oxygen and adsorbed atomic oxygen

k_4 Rate constant for reaction of adsorbed hydroxyl and adsorbed atomic hydrogen

$[O_s]$ Saturation adsorbed oxygen density

$[O_T(t)]$ Total adsorbed oxygen concentration at time "t"

ACKNOWLEDGMENTS

It is a pleasure to acknowledge many stimulating discussions with Richard K. Herz in the early stages of this work and a stimulating discussion with W. Keith Hall who suggested that we verify the isotopic exchange result by checking for exchange between the water product and adsorbed hydrogen at reaction temperature.

REFERENCES

1. Fisher, G. B., Gland, J. L., and Schmieg, S. J., *J. Vac. Sci. Tech.* **20,** 518 (1982).
2. Sexton, B. A., *Surf. Sci.* **94,** 435 (1980).
3. Fisher, G. B., and Gland, J. L., *Surf. Sci.* **94,** 446 (1980).
4. Fisher, G. B., and Sexton, B. A., *Phys. Rev. Lett.* **44,** 683 (1980).
5. Gland, J. L., Sexton, B. A., and Fisher, G. B., *Surf. Sci.* **95,** 587 (1980); Fisher, G. B., Sexton, B. A., and Gland, J. L., *J. Vac. Sci. Technol.* **17,** 144 (1980).
6. Gland, J. L., *Surf. Sci.* **93,** 487 (1980).
7. Christmann, K., Ertl, G., and Pignet, T., *Surf. Sci.* **54,** 365 (1976).
8. Norton, P. R., and Richards, P. J., *Surf. Sci.* **44,** 129 (1974).
9. Baro, A. M., Ibach, H., and Bruckmann, H. D., *Surf. Sci.* **88,** 384 (1979).
10. Norton, P. R., "The Hydrogen–Oxygen Reaction on Metal Surfaces," in preparation.
11. Monroe, D. R., and Merrill, R. P., *J. Catal.* **65,** 461 (1980).
12. Pacia, N., and Dumesic, J. A., *J. Catal.* **41,** 155 (1976).
13. Netzer, F. P., and Kneringer, G., *Surf. Sci.* **51,** 526 (1975).
14. Norton, P. R., *J. Catal.* **36,** 211 (1975).
15. Smith, J. N., and Palmer, R. L., *J. Chem. Phys.* **56,** 13 (1972).
16. Kasemo, B., and Tornqvist, E., *Phys. Rev. Lett.* **44,** 1555 (1980).
17. Ceyer, S. T., Siekhaus, W. J., and Somorjai, G. A., *J. Vac. Sci. Technol.*, in press; Ceyer, S. T., Ph.D. Thesis, University of California, Berkeley, 1979.
18. Tevault, D. E., Talley, L. D., and Lin, M. C., *J. Chem. Phys.* **72,** 3314 (1980).
19. Gland, J. L., and Fisher, G. B., in preparation.
20. Morrow, B. A., and Ramamurthy, P., *J. Phys. Chem.* **77,** 3052 (1973).
21. Engel, T., and Kuipers, H., *Surf. Sci.* **90,** 181 (1979).
22. Yates, J. T., Thiel, P. A., and Weinberg, W. H., *Surf. Sci.* **82,** 45 (1979).
23. Lewis, R., and Gomer, R., *Surf. Sci.* **12,** 157 (1968).